Supporting Information

Synthesis of trimetallic $(HPd@M_2Au_8)^{3+}$ superatoms (M = Ag, Cu) via hydride-mediated regioselective doping to $(Pd@Au_8)^{2+}$

Haru Hirai,[†] Shinjiro Takano,[†] and Tatsuya Tsukuda[†,‡*]

[†]Department of Chemistry, School of Science, The University of Tokyo, Hongo 7-3-1, Bunkyo-Ku, Tokyo 113-0033, Japan

[‡]Elements Strategy Initiative for Catalysts and Batteries (ESICB), Kyoto University, Katsura, Kyoto 615-8520, Japan

1. Experimental Section

Reaction of $[PdAu_8(PPh_3)_8]^{2+}$ and $AgCl(PPh_3)$

A 7-mL screw-capped vial equipped with a magnetic stir bar was charged with $[PdAu_8(PPh_3)_8](NO_3)_2$ (19.5 mg, 5 μmol). The cluster was dissolved in EtOH (500 μL) and diluted with THF (5 mL). A DCM solution of $AgCl(PPh_3)$ (6.1 mg, 15 μmol in 500 μL) was added to the stirred solution. The vial was wrapped in aluminum foil and stirring was continued for 2 h. For ESI-MS and UV-Vis absorption spectroscopy, a small portion of the reaction solution was diluted (ESI-MS: 10 times, UV-Vis absorption spectroscopy: 100 times).

Reaction of $[PdAu_8(PPh_3)_8]^{2+}$ and $CuCl(PPh_3)$

The reaction with copper complex was conducted by the same procedure as that of $AgCl(PPh_3)$, using a DCM solution of $CuCl(PPh_3)$ (5.4 mg, 15 μmol in 500 μL) instead of $AgCl(PPh_3)$. The reaction was conducted under ambient light and an Ar atmosphere.

Coreduction of $AuCl(PPh_3)$, $Pd(PPh_3)_4$, and $AgCl(PPh_3)$

The procedures are based on those used in the synthesis of **1** with modifications.[1] A 15-mL screw-capped test tube equipped with a magnetic stir bar was charged with $AuCl(PPh_3)$ (71.2 mg, 144 μmol), $AgCl(PPh_3)$ (21.9 mg, 54 μmol), and $Pd(PPh_3)_4$ (20.8 mg, 18 μmol). EtOH (5.5 mL) was added to the tube and the solution was stirred to obtain a yellowish white suspension. After stirring for 1 min, a powder of $NaBH_4$ (7.6 mg, 201 μmol) was added and the suspension turned dark brown. The suspension was stirred vigorously for 2 h under dark conditions, and then was poured into hexane (60 mL) through a cotton plug, forming a brown precipitate. The precipitate collected by centrifugation was rinsed with hexane three times and then with 1:1 hexane–DCM. The residue was extracted by DCM and evaporated to dryness. The final product was obtained as a dark brown solid (12.3 mg).

Coreduction of $AuCl(PPh_3)$, $Pd(PPh_3)_4$, and $CuCl(PPh_3)$

The coreduction of $AuCl(PPh_3)$, $Pd(PPh_3)_4$, and $CuCl(PPh_3)$ (19.5 mg, 54 μmol) was

conducted by a similar method to that described above. The reaction was conducted under ambient light and an Ar atmosphere. The final product was obtained as a dark brown solid (8.8 mg).

X-ray absorption fine-structure (XAFS) measurements

Ag K-edge XAFS measurements were conducted at the BL01B1 beamline at the SPring-8 facility of the Japan Synchrotron Radiation Research Institute. The incident X-ray beam was monochromatized by an Si(311) double-crystal monochromator. All XAFS spectra were measured in the fluorescence mode using a 19-element Ge solid-state detector. The X-Ray energy was calibrated using Ag foil. XAFS spectra of $AgClPPh_3$ and **2** were measured in an EtOH-THF (1:10) suspension under stirring. *In situ* XAFS spectrum was measured 20 min after the addition of an EtOH solution of $NaBH_4$ and a DCM solution into an EtOH-THF (10:1) solution of $[PdAu_8(PPh_3)_8](NO_3)_2$. The concentrations of the samples for *in situ* measurement were the same as those for the synthesis of **2**. Data analysis was conducted using the program REX2000 Ver. 2.5.9 program (Rigaku Co.).

Density functional theory (DFT) calculation

Electronic and geometric structures of $[HPdAg_2Au_8(PMe_3)_8Cl_2]^+$ (**2m**) and $[HPdCu_2Au_8(PMe_3)_8Cl_2]^+$ (**3m**) were studied through DFT calculations using the B3LYP functional. Basis sets used were LanL2dz for Pd, Au, Ag, and Cu and 6-31G(d) for Cl, P, C, and H atoms. Singlet spin states were assumed for **2m** and **3m**. Structural optimization was carried out followed by frequency calculations to confirm that the optimized structures had no imaginary frequencies, indicating that they were located at the local/global minima of the potential energy surfaces. Net charges of individual atoms were evaluated by natural population analysis based on natural bond orbitals (NBOs). The relative energies between structural isomers were shown with vibrational zero-point energy corrections. All calculations were conducted using the Gaussian 09 program.[2]

X-ray crystallography

Single-crystals of **2** or **3** were immersed in Paratone-N oil to avoid evaporation of the solvent. A suitable crystal for the diffraction experiment was scooped up and rapidly frozen by a cooled N_2 stream. The diffraction experiment was performed on a Rigaku VariMax dual-wavelength optic/Saturn 724+ diffractometer using MoKα radiation. The data was corrected for Lorentz polarization and absorption correction was done numerically (NUMABS, Rigaku). The initial phase trials were conducted by means of a direct method using SHELXS-2018, and the structures were refined using the full-matrix least-squares method on F^2 by SHELXL-2018.[3] The diffused electron density of the crystal was treated by SQUEEZE on the PLATON platform.[4,5] The counter anion (Cl^- or NO_3^-) has significantly disordered nature in **2**; thus the cluster and solvent molecule were refined for **2** whereas the cluster component and isolated Cl atom were refined for **3**. All non-hydrogen atoms, except for the solvent molecule and isolated Cl atom, were refined anisotropically and the hydrogen atoms were treated as riding models. All aromatic rings were treated using rigid constraints (AFIX 66). As for **2**, no occupancy analysis was needed to refine the structure. In the case of **3**, however, large positive residual electron densities were found on the Cu atoms. To solve this, the occupancy analysis of Cu and Au was conducted using constraints for the coordinates (EXYZ) and the displacement factor (EADP). It was found that the

probable positions of the Cu atoms were only at the chloride coordinated positions. The final occupancy for Cu was 1.68 in **3**, which was in good agreement with the estimated abundance from the $^{31}P\{^{1}H\}$ NMR results. ChcekCif program showed a B-level alert in both crystals for the missing reflections below theta min. Since the crystals have relatively long *c*-axis, some reflections were dumped by direct beam stopper due to the use of MoKα radiation. The lower angle reflections usually affect the interstitial structure such as solvent structure, therefore this alert does not affect the main conclusion of the present study. The structure data was deposited at the Cambridge Crystal Structure Center (CCDC) with the depository numbers 1887210 and 1887211 for **2** and **3**, respectively.

2. Results

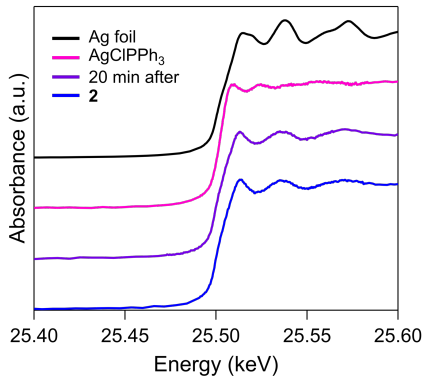

Figure S1. Ag K-edge X-ray absorption near-edge structure spectra of Ag foil, $AgCl(PPh_3)$, **2**, and the spectrum 20 min after the addition of $AgCl(PPh_3)$.

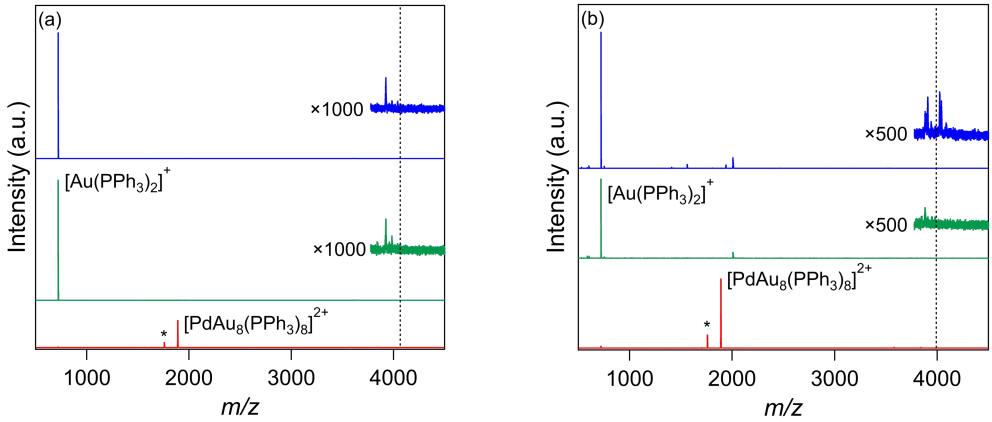

Figure S2. *In situ* positive-ion ESI-MS spectra of the reaction between $[PdAu_8(PPh_3)_8]^{2+}$ and (a) $AgCl(PPh_3)$ or (b) $CuCl(PPh_3)$ before addition of the complex (red), <5 min after addition (green), and 2 h after addition (blue). The dotted lines in panels (a) and (b) correspond to the *m/z* values of **2** and **3**, respectively. The peaks with asterisks are assigned to $[PdAu_8(PPh_3)_7]^{2+}$ generated by in-source collision-induced dissociation.

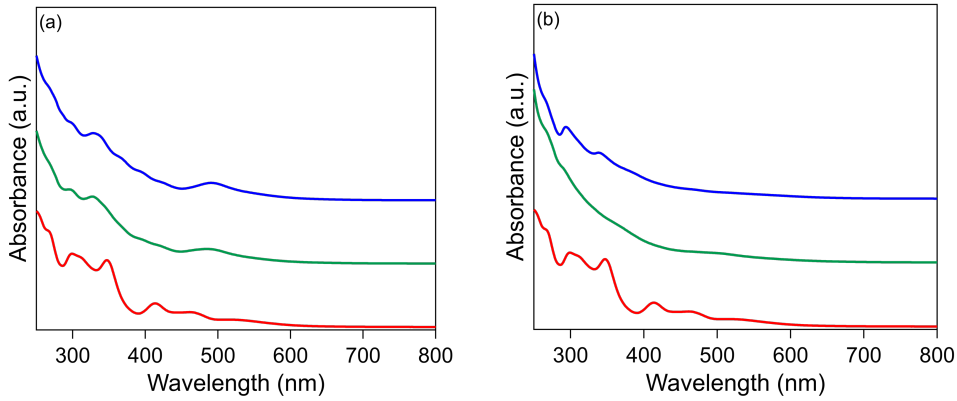

Figure S3. *In situ* UV-Vis absorption spectra of the reaction between $[PdAu_8(PPh_3)_8]^{2+}$ and (a) $AgCl(PPh_3)$ or (b) $CuCl(PPh_3)$ before the addition of the complex (red), <5 min after the addition (green), and 2 h after addition (blue).

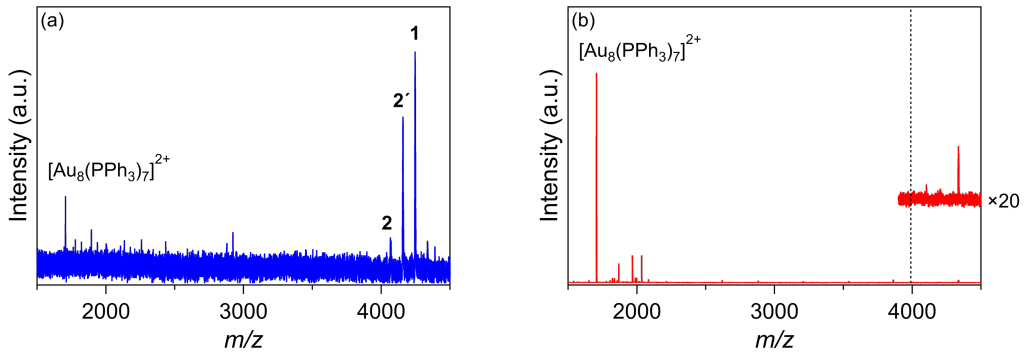

Figure S4. Positive ESI-MS spectra of the final product of coreduction of $AuCl(PPh_3)$ and $Pd(PPh_3)_4$ with (a) $AgCl(PPh_3)$ and with (b) $CuCl(PPh_3)$. The dotted lines in the panel (b) corresponds to the *m/z* value of **3**.

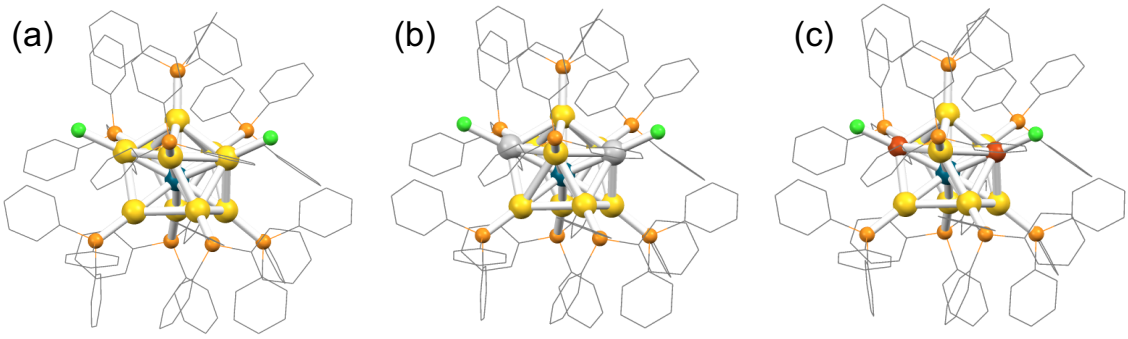

Figure S5. SCXRD structures of (a) **1**, (b) **2**, and (c) **3**. Phenyl groups are depicted as gray wireframes and hydrogen atoms on the phenyl rings are omitted for simplicity. Color codes: yellow (Au); light gray (Ag); brown (Cu); dark green (Pd); blue (H); orange (P); light green (Cl).

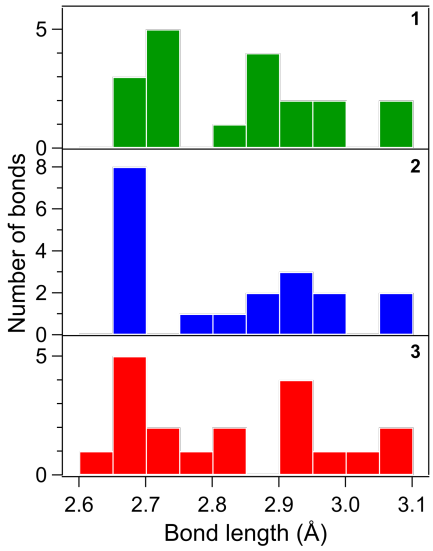

Figure S6. Lengths of the Au–Au bonds between adjacent $AuPPh_3$ units and the radial Pd–Au bonds of **1** (green), **2** (blue), and **3** (red).

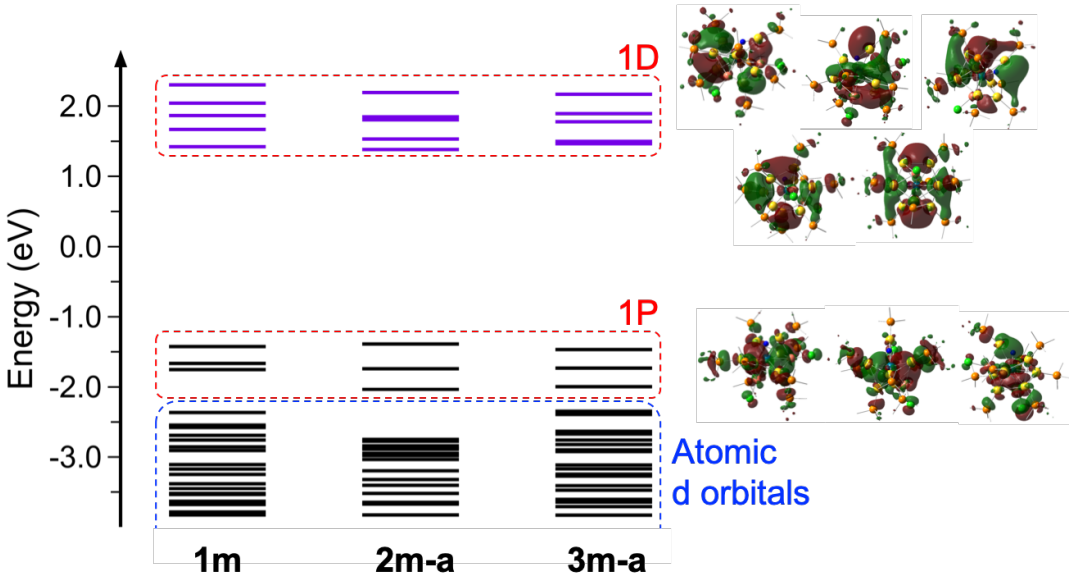

Figure S7. Calculated energy diagrams of **1m**, **2m-a**, and **3m-a**. Black lines correspond to energy levels of occupied orbitals and purple ones correspond to those of unoccupied orbitals. The energies are referenced to the middle of the HOMO-LUMO gap of each cluster. Kohn-Sham orbitals of **3m-a** were depicted with isodensity values at the 0.02e level. Methyl groups are depicted as gray wireframes. Color codes: yellow (Au); brown (Cu); dark green (Pd); blue (H); orange (P); light green (Cl).

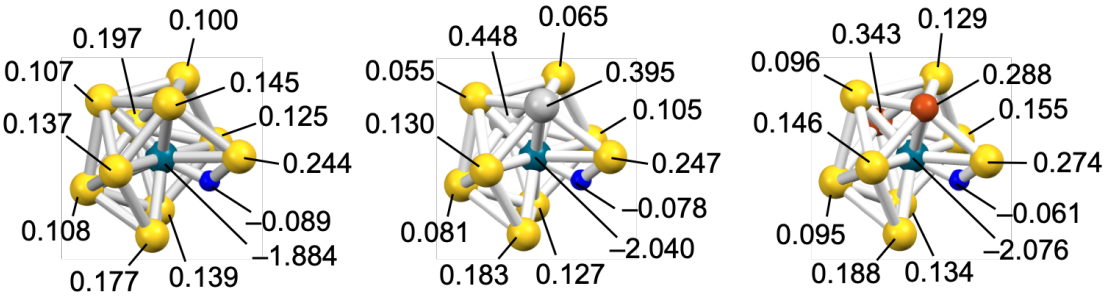

Figure S8. NBO charges of the individual atoms of **1m**, **2m-a**, and **3m-a**. Color codes: yellow (Au); light gray (Ag); brown (Cu); dark green (Pd).

Table S1. Crystal data of **2**·(*i*-Pr)$_2$O.

Formula[a]	$C_{150}H_{134}Ag_2Au_8Cl_2O_1P_8Pd_1$
FW[a] (g mol^{-1})	4169.10
Crystal size (mm)	0.08 x 0.07 x 0.02
Crystal system	Monoclinic
Space group, Z	$P2_1/c$, 4
a (Å)	22.158(3)
b (Å)	18.750(2)
c (Å)	34.486(5)
β (°)	97.785(3)
V (Å^3)	14196(3)
T (K)	93(2)
ρ_{calc} (g cm^{-3})	1.951
μ (mm^{-1})	8.802
θ range (°)	2.5 – 25.4
Measured reflections	203206
Unique reflections	25988 (R_{int} = 0.0748)
Data/restrains/parameters	25988/237/1226
R[b,c] indices [$I > 2\sigma(I)$]	R_1 = 0.0900, wR_2 = 0.1629
R[b,c] indices [all data]	R_1 = 0.0966, wR_2 = 0.1658
Goodness-of-fit on F^2	1.281

[a] Including solvent molecules. [b] $R_1 = \Sigma(||F_o| - |F_c||)/\Sigma|F_o|$. [c] $wR_2 = [\Sigma[w(F_o^2 - F_c^2)^2]/\Sigma[w(F_o^2)^2]]^{1/2}$, $w = 1/[\sigma^2(F_o^2) + (ap)^2 + bp]$, where $p = [\max(F_o^2, 0) + 2F_c^2]/3$.

Table S2. Crystal data of **3**·Cl.

Formula[a]	$C_{144}H_{120}Cu_2Au_8Cl_3P_8Pd_1$
FW[a] (g mol^{-1})	4013.72
Crystal size (mm)	0.12 x 0.04 x 0.01
Crystal system	Monoclinic
Space group, Z	$P2_1/c$, 4
a (Å)	22.193(4)
b (Å)	18.278(3)
c (Å)	34.743(6)
β (°)	96.765(3)
V (Å^3)	13995(4)
T (K)	93(2)
ρ_{calc} (g cm^{-3})	1.905
μ (mm^{-1})	8.843
θ range (°)	2.1 – 25.3
Measured reflections	148200
Unique reflections	25581 (R_{int} = 0.1013)
Data/restrains/parameters	25581/468/1214
R[b,c] indices [$I > 2\sigma(I)$]	R_1 = 0.1013, wR_2 = 0.1717
R[b,c] indices [all data]	R_1 = 0.1177, wR_2 = 0.1788
Goodness-of-fit on F^2	1.234

[a] Including solvent molecules. [b] $R_1 = \Sigma(||F_o| - |F_c||)/\Sigma|F_o|$. [c] $wR_2 = [\Sigma[w(F_o^2 - F_c^2)^2]/\Sigma[w(F_o^2)^2]]^{1/2}$, $w = 1/[\sigma^2(F_o^2) + (ap)^2 + bp]$, where $p = [\max(F_o^2, 0) + 2F_c^2]/3$.

References

(1) Kurashige, W.; Negishi, Y. Synthesis, Stability, and Photoluminescence Properties of $PdAu_{10}(PPh_3)_8Cl_2$ Clusters. *J. Cluster Sci.* **2012**, *23*, 365–374.

(2) Frisch, M. J.; Trucks, G. W.; Schlegel, H. B.; Scuseria, G. E.; Robb, M. A.; Cheeseman, J. R.; Scalmani, G.; Barone, V.; Mennucci, B.; Petersson, G. A.; Nakatsuji, H.; Caricato, M.; Li, X.; Hratchian, H. P.; Izmaylov, A. F.; Bloino, J.; Zheng, G.; Sonnenberg, J. L.; Hada, M.; Ehara, M.; Toyota, K.; Fukuda, R.; Hasegawa, J.; Ishida, M.; Nakajima, T.; Honda, Y.; Kitao, O.; Nakai, H.; Vreven, T.; Montgomery, J. A., Jr.; Peralta, J. E.; Ogliaro, F.; Bearpark, M.; Heyd, J. J.; Brothers, E.; Kudin, K. N.; Staroverov, V. N.; Kobayashi, R.; Normand, J.; Raghavachari, K.; Rendell, A.; Burant, J. C.; Iyengar, S. S.; Tomasi, J.; Cossi, M.; Rega, N.; Millam, J. M.; Klene, M.; Knox, J. E.; Cross, J. B.; Bakken, V.; Adamo, C.; Jaramillo, J.; Gomperts, R.; Stratmann, R. E.; Yazyev, O.; Austin, A. J.; Cammi, R.; Pomelli, C.; Ochterski, J. W.; Martin, R. L.; Morokuma, K.; Zakrzewski, V. G.; Voth, G. A.; Salvador, P.; Dannenberg, J. J.; Dapprich, S.; Daniels, A. D.; Farkas, Ö.; Foresman, J. B.; Ortiz, J. V.; Cioslowski, J.; Fox, D. J. Gaussian 09, Revision D.01, Gaussian, Inc., Wallingford CT, 2013.

(3) Sheldrick, G. M. Crystal Structure Refinement with *SHELXL*. *Acta Cryst. C* **2015**, *71*, 3–8.

(4) Van der Sluis, P.; Spek, A. L. BYPASS: an Effective Method for the Refinement of Crystal Structures Containing Disordered Solvent Regions. *Acta Cryst. A* **1990**, *46*, 194–201.

(5) Spek, A. L. Single-Crystal Structure Validation with the Program *PLATON*. *J. Appl. Cryst.* **2003**, *36*, 7–13.